Actin-regulated feedback loop based on Phactr4, PP1 and cofilin maintains the actin monomer pool

Guillaume Huet[1,*], Eeva Kaisa Rajakylä[1,*], Tiina Viita[1,*], Kari-Pekka Skarp[1], Marko Crivaro[2], Joseph Dopie[1] and Maria K. Vartiainen[1,‡]

[1]Program in Cell and Molecular Biology, Institute of Biotechnology, University of Helsinki, 00014 Finland
[2]Light Microscopy Unit, Institute of Biotechnology, University of Helsinki, 00014 Finland

*These authors contributed equally to this work
‡Author for correspondence (maria.vartiainen@helsinki.fi)

Accepted 12 November 2012
Journal of Cell Science 126, 497–507

doi: 10.1242/jcs.113241

Summary

Phactr proteins bind actin and protein phosphatase 1 (PP1), and are involved in processes ranging from angiogenesis to cell cycle regulation. Phactrs share a highly conserved RPEL domain with the myocardin-related transcription factor (MRTF) family, where actin binding to this domain regulates both the nuclear localization and the activity of these transcription coactivators. We show here that in contrast to MRTF-A, the RPEL domain is dispensable for the subcellular localization of Phactr4. Instead, we find the domain facilitating competitive binding of monomeric actin and PP1 to Phactr4. Binding of actin to Phactr4 influences the activity of PP1 and the phosphorylation status of one of its downstream targets, cofilin. Consequently, at low actin monomer levels, Phactr4 guides PP1 to dephosphorylate cofilin. This active form of cofilin is then able to sever and depolymerize actin filaments and thus restore the actin monomer pool. Accordingly, our data discloses the central role of Phactr4 in a feedback loop, where actin monomers regulate their own number via the activation of a key regulator of actin dynamics. Depending on the protein context, the RPEL domain can thus elicit mechanistically different responses to maintain the cellular actin balance.

Key words: RPEL domain, Actin, Protein phosphatase 1, Phactr, Cofilin

Introduction

The actin cytoskeleton plays many important roles in the cell for example in the context of cell migration. Controlled formation of actin filaments is responsible for most actin-dependent cellular processes, but the maintenance of an unpolymerized monomer pool is equally important to ensure the continuous supply of actin monomers to the sites of active polymerization. Therefore, cells contain a large number of proteins, which regulate the size and dynamics of the actin monomer pool (Paavilainen et al., 2004).

There are also proteins that use actin monomer levels as a signalling intermediate. The RPEL domain is a conserved protein domain present in two protein families: the phosphatase and actin regulating proteins (Phactrs), consisting of Phactr1, Phactr2, Phactr3/scapinin and Phactr4 and the myocardin-related transcription factor family (MRTFs), with myocardin, MRTF-A (MAL/MKL1) and MRTF-B (MKL2). MRTFs are coactivators of serum response factor (SRF), which is an essential transcription factor in control of many immediate-early, cytoskeletal and muscle specific genes. With the exception of Myocardin, the RPEL domain in MRTFs seems to bind actin (Guettler et al., 2008; Miralles et al., 2003; Vartiainen et al., 2007). The RPEL domain of MRTF-A consists of three RPEL motifs of 22 amino acids organized around the core consensus sequence RPxxxEL (arginine R, proline P, any amino acid x, glutamate E and leucine L). Each RPEL motif functions as an actin-binding element (Guettler et al., 2008) but also the linker sequences separating the motifs contribute to the binding (Mouilleron et al., 2011). The RPEL domain is both necessary and sufficient for controlling the nucleo-cytoplasmic shuttling of MRTF-A in response to actin dynamics. MRTF-A constantly shuttles in and out of the nucleus (Vartiainen et al., 2007). At high actin monomer levels, actin-binding to the RPEL domain masks the nuclear localization signal (NLS), comprised of basic regions B2 and B3, thus preventing nuclear import of MRTF-A (Mouilleron et al., 2011; Pawlowski et al., 2010). Actin-binding is also required for efficient nuclear export of MRTF-A (Vartiainen et al., 2007). The structural basis for neither this nor the actual nuclear export sequences (NES) have been characterized. In addition, actin-binding in the nucleus seems to prevent MRTF-A from activating SRF-mediated transcription (Vartiainen et al., 2007). Decreased actin monomer levels will therefore result in nuclear localization of active MRTF-A. Hence, the RPEL domain allows MRTF-A to function as an actin monomer sensor and to regulate gene expression according to actin dynamics. As many SRF targets are cytoskeletal genes (Sun et al., 2006), this creates a feedback loop, where actin dynamics regulate the expression of its components.

The functional role of the RPEL domain in Phactr proteins is unknown although it appears to mediate actin-binding also in this protein family (Allen et al., 2004; Favot et al., 2005; Sagara et al., 2009). In addition to actin, the differently expressed Phactr family members interact with protein phosphatase 1 (PP1) (Allen et al., 2004; Kim et al., 2007; Sagara et al., 2003), with their highly conserved C-terminal tail (Fig. 1A), which starts immediately after the last RPEL motif. The subcellular localization of Phactr proteins

Journal of Cell Science

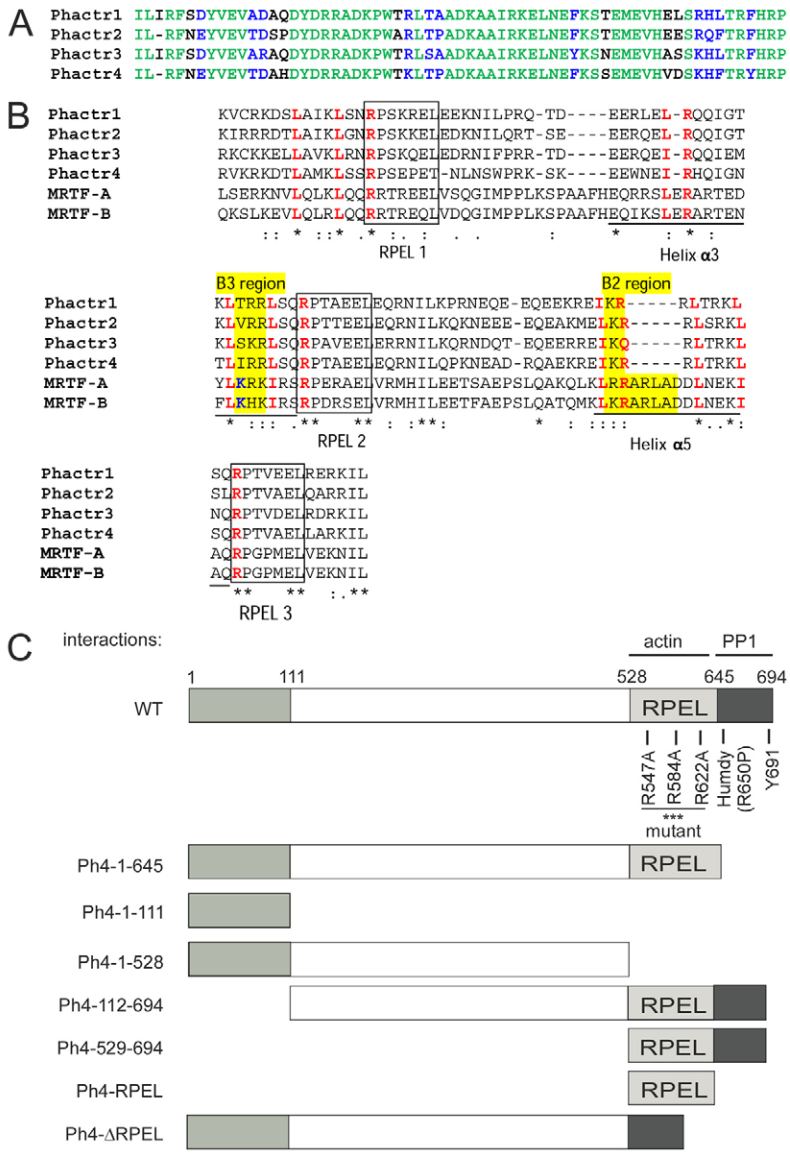

Fig. 1. Structural aspects of Phactr proteins. (**A**) Alignment with the ClustalW2 program of the PP1 binding tails of mouse Phactr proteins 1 to 4 depicting their high homology (87% identical). Perfectly identical amino acids are shown in green and those that share a high homology of size and charge in blue. (**B**) Sequences of RPEL domains of mouse Phactr1, 2, 3 and 4 as well as MRTF-A and MRTF-B were aligned using the ClustalW2 software. Positions of MRTF RPEL α3 and α5 helices are underlined. The position corresponding to B2 and B3 regions in MRTF-A are in yellow. RPEL motifs are in blue. The main amino acids involved in actin binding (Mouilleron et al., 2011) are in bold red. Amino acid conservation is shown below the sequences. Asterisks (*) indicate perfect identity in all sequences, colons (:) and periods (.) indicate a strong or weak homology, respectively. (**C**) Schematic representation of Phactr4 constructs used in the study. The regions involved in interactions are indicated above the representation of the wild-type (WT) Phactr4, as well as the numbers of the amino acids delimiting the different regions described in the protein. The position of the RPEL domain as well as amino acid subjects of point mutations in Phactr***, humdy (R650P) and Y691A are indicated. The different deletion mutants are represented below. Numbers in the names indicate amino acids included in the construct.

has not been studied systematically and variable localization patterns ranging from nuclear to cytoplasmic have been reported (Allen et al., 2004; Farghaian et al., 2011; Favot et al., 2005; Kim et al., 2007; Sagara et al., 2009; Sagara et al., 2003; Zhang et al., 2012). Phactr proteins have been implicated in many distinct biological processes, from angiogenesis (Allain et al., 2012; Jarray et al., 2011) to cell spreading, migration (Sagara et al., 2009) and axon elongation (Farghaian et al., 2011), which are also dependent on the actin cytoskeleton. Mice carrying a specific mutation of *Phactr4* gene called the *humdy* exhibit a defect of neural tube and optic fissure closure resulting in anomalies such as exencephaly. The Phactr4 *humdy* mutant (R650P) cannot interact with PP1, resulting in abnormal phosphorylation of retinoblastoma protein, a crucial cell cycle regulator (Kim et al., 2007). The *humdy* mutation also seems to impair directional migration of enteric neural crest cells, likely due to defects in actin cytoskeleton regulation through both integrin signalling and cofilin activity (Zhang et al., 2012). Therefore, most of the biological functions of Phactr proteins described so far involve either actin or PP1 but the interplay between these two Phactr interactions has not been explored.

As the RPEL domain of Phactrs is highly similar to the RPEL domain in MRTFs, we decided to investigate whether the RPEL domains function similarly in these two protein families. We show that unlike in MRTF-A, the RPEL domain does not play a role in controlling the subcellular localization of Phactr4. Most importantly, we demonstrate that actin-binding to Phactr4 RPEL domain controls, through a competition mechanism, the binding of Phactr4 to one of its key targets, PP1 and consequently the phosphatase activity of this enzyme. We show that in cells this mechanism can be used to fine-tune actin monomer levels through a feedback loop, where actin monomer-binding to Phactr4 RPEL domain controls, through PP1, the phosphorylation status and thus activity of the key actin disassembly factor cofilin. Taken together, our data reveals a novel role for the RPEL domain in the regulation of a key enzymatic activity according to the ratio of monomeric and polymeric actin in cells.

Results

Localization of Phactr proteins in mammalian cells

The functional significance of the RPEL domain in Phactr proteins has not been established, although it is known that in MRTF-A, the RPEL domain is both necessary and sufficient to regulate the subcellular localization of the protein. To systematically assess if this is the case also in Phactr proteins, we expressed each member of the Phactr family, Phactr1, 2, 3 and 4 fused to the green fluorescent protein (GFP) at their N-terminus and compared their localization to MRTF-A-GFP in NIH 3T3 cells, which have been extensively used to study MRTF-A regulation (Miralles et al., 2003; Vartiainen et al., 2007). In unstimulated (serum-starved) cells, MRTF-A-GFP was cytoplasmic in most cells (Fig. 2) as established previously (Miralles et al., 2003; Vartiainen et al., 2007). In these conditions, most Phactr proteins exhibited diffuse localization in cells (Fig. 2A) and all of them also appeared to localize to the plasma membrane (see also Fig. 3). We then made a direct comparison of the number of cells that exhibit a clearly cytoplasmic, a clearly nuclear or diffuse localization with the boundary of nucleus and cytoplasm indistinguishable, as established previously for scoring MRTF-A localization (Vartiainen et al., 2007). In unstimulated conditions, all four Phactr proteins showed a very similar distribution with majority of cells scoring as diffusely localized (Fig. 2B). Phactr2 appeared more frequently mainly in the cytoplasm and Phactr1 and Phactr3 displayed a slightly higher nuclear distribution than the other family members (Fig. 2B). Of note, overexpression of any of the Phactr proteins resulted in changes in cell morphology as also reported earlier (Favot et al., 2005) and we were therefore very careful to exclude highly expressing cells with distorted morphology. Thus, Phactr proteins have a less striking distribution than MRTF-A in low-serum conditions. Because Phactr4 is the most expressed family member in the NIH 3T3 cells according to our preliminary quantitative RT-PCR analysis, we chose this member of the Phactr family for further investigation. To ensure that the GFP does not interfere with the localization of the Phactr proteins, we also examined Phactr4

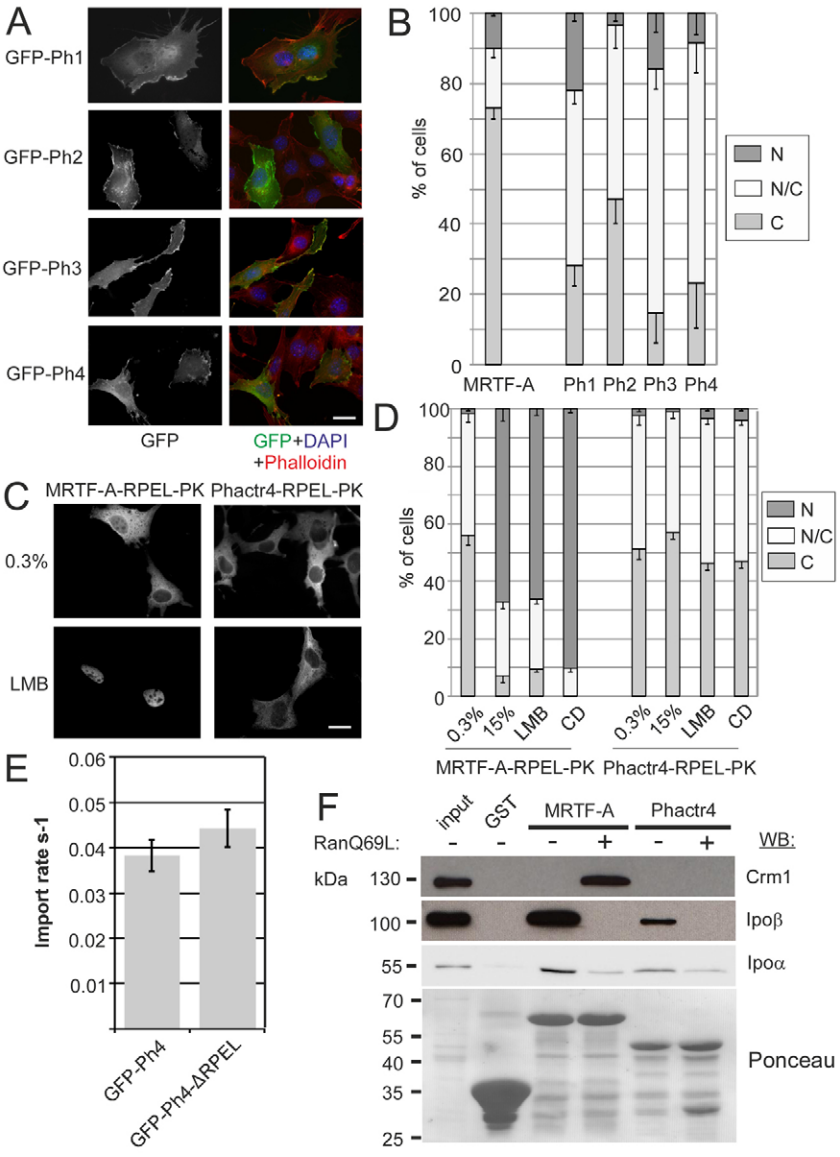

Fig. 2. Phactr protein localization does not respond to same stimuli as MRTF-A does and the RPEL domain does not mediate regulated nucleo-cytoplasmic shuttling of Phactr4. (**A**) Fluorescence microscopy images of NIH 3T3 cells expressing GFP-tagged Phactr1 (Ph1), Phactr2 (Ph2), Phactr3 (Ph3) and Phactr4 (Ph4) in unstimulated, 0.3% serum condition. Right: merged image with GFP (green), phalloidin (red) and DAPI (blue). (**B**) Quantification of the proportion of cells that exhibit a clearly nuclear (N), cytoplasmic (C) or undistinguishable signal between nucleus and cytoplasm (N/C); 100 cells per construct, $n=3$; error bars indicate s.e.m. (**C**) Fluorescence microscopy images of cells expressing the RPEL domains of MRTF-A (MRTF-A-RPEL-PK) or Phactr4 (Phactr4-RPEL-PK) fused to chicken pyruvate kinase (PK), grown in low serum conditions (0.3%) and treated or not with 20 nM leptomycin B (LMB). (**D**) Quantification of the distribution of MRTF-A-RPEL-PK and Phactr4-RPEL-PK constructs in specified conditions; 100 cells per construct, $n=3$; error bars indicate s.e.m. (**E**) Import rate of GFP-Phactr4 (GFP-Ph4) and GFP-Phactr4-ΔRPEL (GFP-Ph4-ΔRPEL) measured by FRAP; data represent mean import rates ± s.d. ($n=8$ and 10, respectively). (**F**) GST pull-down of importin α (Ipoα), importin β (Ipoβ) and Crm1 from a HeLa cell lysate using MRTF-A or Phactr4 RPEL domains fused to GST as baits, in the presence (+) or absence (−) of Ran-Q69L, analyzed by western blot (WB). Input samples correspond to 5% of the HeLa cell lysate used in the assay. Ponceau staining ensures equal loading of samples. Scale bars: 20 μm.

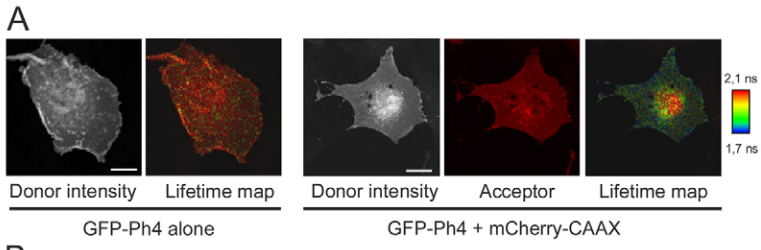

B

Donor and acceptor combination	GFP average lifetime (ns)	Standard deviation (ns)	Average FRET efficiency
GFP	2.118	0.030	
GFP+Che (negative control)	2.118	0.011	0.0 %
Che-GFP tandem (positive control)	1.846	0.022	12.86 %
GFP-Ph4	2.133	0.015	
GFP-Ph4 + Che-CAAX	1.846	0.039	13.42 %
GFP-Ph4-1-111	2.049	0.024	
GFP-Ph4-1-111 + Che-CAAX	1.883	0.055	8.11 %
GFP-Ph4-112-694	2.092	0.021	
GFP-Ph4-112-694 + Che-CAAX	1.991	0.026	4.84 %
GFP-Ph4-529-694	2.165	0.005	
GFP-Ph4-529-694 + Che-CAAX	2.131	0.007	1.56 %

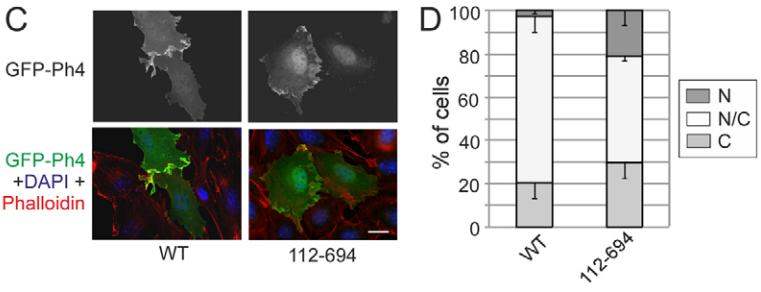

Fig. 3. Phactr4 localizes to the plasma membrane. (**A**) FRET/FLIM between GFP-Ph4 (donor) and mCherry-CAAX (acceptor) was used to study membrane targeting of Phactr4. Microscopy images show the intensity images of the donor and acceptor and the lifetime map of the donor in the absence (left) or presence (right) of the acceptor. The lifetime map is color coded according to the key on the right. (**B**) Quantification of donor fluorescence lifetime of the indicated samples. The FRET efficiency was calculated as described in Materials and Methods. Data are from at least nine cells, from three independent experiments. (**C**) Fluorescence microscopy image of cells expressing GFP-Phactr4 (WT) or GFP-Phactr4-112–694 (112–694). Lower panel shows the merged image with GFP (green), DAPI (blue) and phalloidin (red). (**D**) Quantification of the localization of the constructs indicated in C; 100 cells per construct, $n=3$; error bars indicate s.e.m. Scale bars: 20 µm.

with GFP fused in the C-terminus of the protein or with a shorter FLAG-epitope tag. Both of these constructs localized very similarly to the N-terminally GFP-tagged Phactr4 (data not shown), demonstrating that the GFP-fusion is likely a good probe for studying Phactr localization in cells.

The RPEL domain of Phactr4 does not control its nuclear localization

Next, we examined the localization of Phactr4 under conditions that are known to modulate the localization of MRTF-A (Miralles et al., 2003; Vartiainen et al., 2007). However, none of our treatments had an effect on Phactr4 localization (data not shown). This result suggests Phactr4 is equipped with the RPEL domain for a purpose other than cellular localization. To test this hypothesis directly, we fused the C-terminal part of Phactr4 that contains the RPEL domain (amino acids 529–645) to a neutral protein, pyruvate kinase, which contains neither NLS nor NES (Kalderon et al., 1984). The MRTF-A-RPEL domain alone is able to drive the nucleo-cytoplasmic localization of pyruvate kinase in the same way as it controls the full length MRTF-A (Guettler et al., 2008). In unstimulated conditions, both RPEL-PK constructs displayed mainly cytoplasmic localization (Fig. 2C,D). Disrupting the actin-MRTF-A complex either through serum stimulation, which induces actin polymerization, or directly by cytochalasin D (Vartiainen et al., 2007) result in nuclear localization of MRTF-A-RPEL-PK (Fig. 2D), as reported before (Guettler et al., 2008). However, these treatments had no effect on Phactr4-RPEL distribution in cells (Fig. 2D). Finally, we treated cells with leptomycin B (LMB), which is a specific inhibitor of Crm1 (Fornerod et al., 1997), the known export receptor for MRTF-A (Vartiainen et al., 2007). Despite the fact that LMB efficiently triggered MRTF-A-RPEL nuclear accumulation (Fig. 2C,D), it did not affect Phactr4-RPEL distribution (Fig. 2C,D), strongly suggesting that MRTF-A and Phactr4 do not share the same mechanism for active nuclear export. Therefore, the distribution of Phactr4 between the cytoplasm and the nucleus is not affected by the same stimuli that redistribute MRTF-A.

We further studied how GFP-Phactr4 is imported into the nucleus in living cells by using a Fluorescence Recovery After Photobleaching (FRAP) assay. In this assay, nucleus is bleached void of fluorescence and the recovery of fluorescence, which is due to the non-bleached molecules entering the nucleus from the cytoplasm, is observed. The initial recovery, when nuclear re-export is still negligible, can then be used as a measure of nuclear import (Dopie et al., 2012). The nuclear fluorescence of GFP-Phactr4 was efficiently recovered after photobleaching (Fig. 2E), demonstrating the continuous input of this protein into the

nucleus. Importantly, deletion of the RPEL domain (GFP-Phactr4-ΔRPEL, see Fig. 1C for constructs used in the study) did not decrease the nuclear import rate (Fig. 2E). This demonstrates that the NLS in Phactr4 does not reside within the RPEL domain and further underscores the notion that the RPEL domain likely plays a different role in Phactr4 than in MRTF family members.

In MRTF-A the RPEL domain contains the binding sites for both the nuclear import and export receptors, importin α/β (Pawlowski et al., 2010) and Crm1 (Guettler et al., 2008; Vartiainen et al., 2007), respectively. We performed GST-pull down assays from cytoplasmic HeLa cell extracts using the RPEL domains of Phactr4 or MRTF-A as baits. In our assay and under similar experimental conditions, both importin α and importin β bound more efficiently to MRTF-A-RPEL than to Phactr4-RPEL (Fig. 2F). Addition of Ran-GTP, which in the nucleus acts to disrupt importin-cargo complexes (Görlich et al., 1996), impaired the pull-down of importins, demonstrating the specificity of the interactions. In addition, Phactr4-RPEL does not pull down MRTF-A export receptor Crm1 under conditions where the MRTF-A-RPEL bound efficiently to it (Fig. 2F). The decreased binding to import and export receptors likely explains why the RPEL domain fails to regulate nucleo-cytoplasmic shuttling of Phactr4.

The N-terminus of Phactr4 targets it to the plasma membrane

Examining the localization of GFP-Phactr4 with a wide-field fluorescence microscope indicated that the protein might be localized to the plasma membrane. We co-expressed GFP-Phactr4 and the membrane localization peptide CAAX fused to the mCherry fluorophore [mCherry-CAAX (van Rheenen et al., 2007)], and measured the Förster Resonance Energy transfer between the GFP and mCherry moieties by using Fluorescence Lifetime Imaging (FLIM). Plasma membrane localization would bring the GFP-Phactr4 in the proximity of the mCherry and permit FRET, which will decrease the fluorescence lifetime of the GFP donor fluorophore. The average lifetime of GFP-Phactr4 alone was 2.13 nanoseconds and it decreased to 1.85 nanoseconds upon co-expression of mCherry-CAAX (Fig. 3A,B), indicating that a fraction of Phactr4 is indeed in a very close proximity to the plasma membrane. Importantly, the C-terminal half of Phactr4, GFP-Ph4-529–694 (see Fig. 1C), failed to produce a FRET signal with mCherry-CAAX (Fig. 3B), proving the specificity of our assay and also suggesting that the plasma membrane targeting signal is in the N-terminal half of the protein. As all Phactr proteins appeared to localize to the plasma membrane (Fig. 2A), we reasoned that the targeting signal may be a conserved feature. Although less conserved than the C-terminus, there is a batch of basic residues in the very N-terminus of all four Phactr proteins (Allen et al., 2004). Deletion of the N-terminal 111 amino acids resulted in a marked decreased in the FRET efficiency between GFP-Ph4-112–694 and mCherry-CAAX (Fig. 3B), indicating that the N-terminus contributes to the plasma membrane targeting but does not exclude the need for other sequences. Importantly, this region alone, GFP-Ph4-1–111, was efficiently targeted to the plasma membrane, and exhibited 8.11% FRET efficiency with the Che-CAAX construct (Fig. 3B). Interestingly, the GFP-Ph4-112–694 mutant lacking the major plasma membrane targeting signals exhibited a more nuclear distribution than the wild-type protein (Fig. 3C,D), suggesting that releasing Phactr4 from the plasma membrane permits its nuclear accumulation.

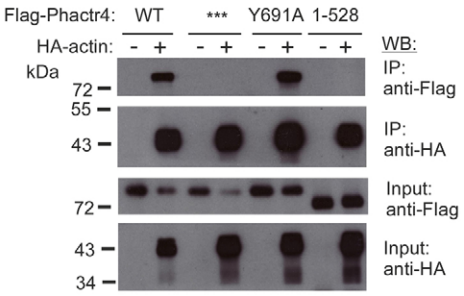

Fig. 4. Same mutations disrupt Phactr4 and MRTF-A binding to actin. Co-immunoprecipitation with anti-HA beads of indicated FLAG-Phactr4 mutants in the presence or absence of HA-tagged actin (HA-actin), analyzed by western-blotting (WB). IP, immunoprecipitation samples. Inputs represent 5% of total protein lysate in IP.

Phactr4 regulates the phosphatase activity of PP1 under the control of actin

Actin-binding to the RPEL domain is a key feature in regulating the subcellular localization of MRTF-A. To confirm the previously published results that Phactr4 binds actin (Favot et al., 2005; Kim et al., 2007), we first performed co-immunoprecipitations, which clearly demonstrate this relationship (Fig. 4). The binding requires the RPEL domain, because deletion of the C-terminus (mutant 1–528) abolished the interaction. In addition, mutation of this domain on three key amino acids corresponding to those required for actin binding in MRTF-A (Guettler et al., 2008; Vartiainen et al., 2007) (Phactr4***), abolished actin binding (Fig. 4), suggesting that Phactr4 and MRTF-A may use a similar mechanism to interact with actin.

We performed further co-immunoprecipitation assays to study how Phactr4 interacts with PP1. We observed an interaction between Phactr4 and all four PP1 isoforms, PP1α, PP1β, PP1γ1 and PP1γ2 (Fig. 5A). As described by others (Allen et al., 2004; Kim et al., 2007; Sagara et al., 2003), the binding of Phactr4 to PP1α requires the C-terminal tail as the deletion mutant lacking either the whole C-terminus, Ph4-1–528, or lacking only sequences after the RPEL domain, Ph4-1–645, failed to interact with PP1 in our assay (Fig. 5B). Within this C-terminal tail, two mutations, R650P and Y691A, 41 amino acids apart, have been described to mediate PP1 binding to Phactrs (Allen et al., 2004; Kim et al., 2007). Under our experimental conditions, both of these mutations prevented the interaction between Phactr4 and PP1 (Fig. 5B), suggesting that the integrity of this whole tail may be important for the binding. Interestingly, the Phactr4 mutant that cannot bind actin (Phactr4***; see Fig. 4) seemed to interact better with PP1 than the wild-type protein (Fig. 5B), suggesting that actin and PP1 may compete for binding to Phactr4.

To directly test this, we next examined the binding of PP1 to Phactr4 in the presence of increasing amounts of purified actin. In support of our hypothesis, the amount of Phactr4 that co-immunoprecipitated with PP1α decreased in a dose-dependent manner by addition of exogenous actin to the reaction (Fig. 5C). Importantly, binding of PP1 to the Phactr4 mutant that does not interact with actin (Phactr4***), was not affected by actin (Fig. 5C). The function of the RPEL domain of Phactr proteins

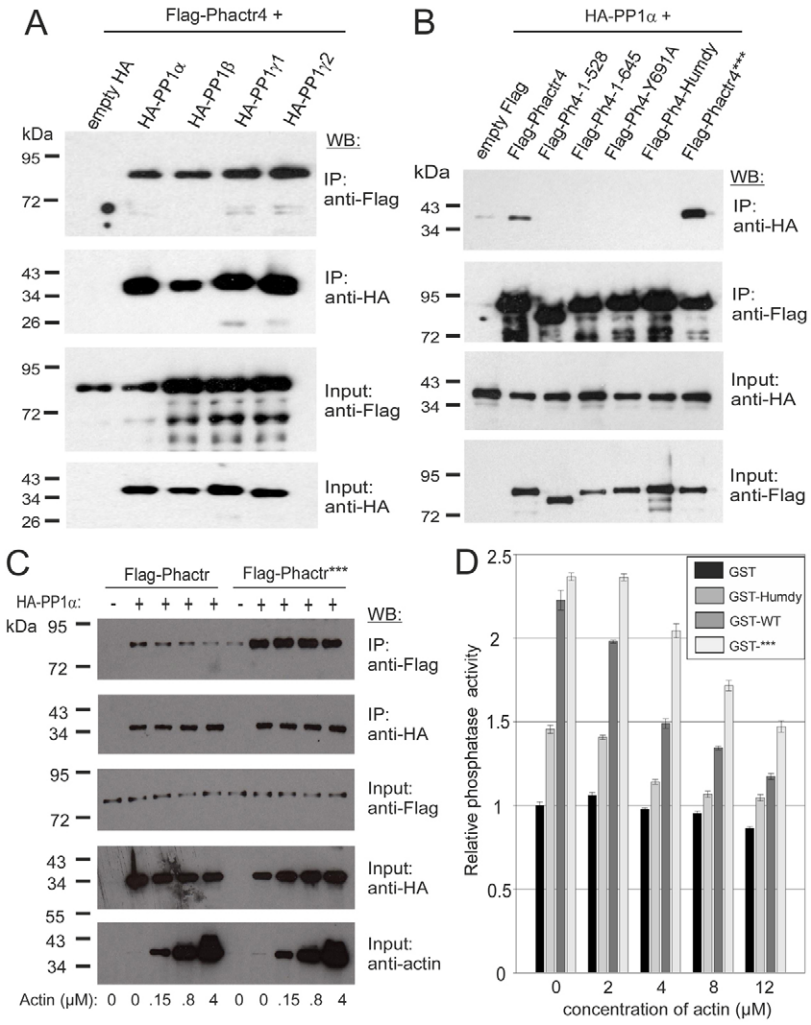

Fig. 5. Actin regulates PP1 activity by competing with PP1 binding to Phactr4. (**A**) Co-immunoprecipitation with anti-HA beads of FLAG-Phactr4 by HA-tagged PP1 isoforms (PP1α, β, γ1 and γ2) analyzed by western blotting (WB). IP, immunoprecipitated samples. (**B**) Co-immunoprecipitation with anti-FLAG beads of indicated FLAG-Phactr4 mutants by HA-PP1α. (**C**) Co-immunoprecipitation with anti-HA beads of FLAG-Phactr4 or FLAG-Phactr4*** with empty HA-plasmid (−) or HA-PP1α (+) in the presence of increasing amounts of exogenous actin. (**D**) *In vitro* PP1 activity in the presence of GST or different GST-Phactr4-529–694 constructs: wild-type (GST-WT), humdy (GST-Humdy) or Phactr4*** (GST-***), with indicated concentrations of purified actin. Data represent the relative phosphatase activity compared to activity with GST minus actin. Data show the mean and s.e.m. of at least three independent experiments.

may therefore be to regulate the binding to PP1 and subsequently control PP1 phosphatase activity through Phactrs. We measured phosphatase activity of PP1α catalytic subunit *in vitro* in the presence or absence of Phactr C-terminal region, Ph4-529–694, while increasing the amount of actin in the mixture. In the absence of Phactr4, PP1 activity remained constant when actin was added (Fig. 5D). The presence of Ph4-529–694 enhanced the phosphatase activity of PP1 catalytic subunit and the addition of actin abolished this enhancement in a dose-dependent manner. In this assay, Phactr4*** was substantially less affected by actin than the wild-type protein (Fig. 5D). Moreover, Phactr4-humdy, which displays decreased binding to PP1 (Fig. 5B) (Kim et al., 2007) failed to increase PP1 activity as efficiently as the wild-type protein (Fig. 5D).

Taken together, the RPEL domain of Phactr4 does not regulate its nucleo-cytoplasmic distribution. Instead, it senses actin concentration and therefore controls, according to actin dynamics, the catalytic activity of PP1.

Actin monomer levels control the phosphorylation of cofilin through Phactr4 and PP1

It was recently reported that the *humdy* mutant mouse with abolished interaction between Phactr4 and PP1 (Kim et al., 2007), displayed elevated levels of phosphorylated cofilin (Zhang et al., 2012). As our data implicated that actin monomer levels control PP1 activity through Phactr4, we decided to test if phosphorylation of cofilin would be regulated through this pathway. Overexpression of the Phactr4-humdy mutant led to increased levels of phospho-cofilin (Fig. 6A,B), as expected (Zhang et al., 2012). Interestingly, expression of the unpolymerizable actin mutant R62D, which will bind to Phactr4 and prevent it from activating PP1, also resulted in increased phospho-cofilin (Fig. 6B). Overexpression of wild-type Phactr4 (Fig. 6A,B) or Phactr4*** led to decreased phospho-cofilin levels (Fig. 6B). This decrease was dependent on phosphatase activity, because the effect could be reversed with okadaic acid. Importantly, coexpression of the actin mutant R62D reversed the effect of the wild-type Phactr4 on phospho-cofilin levels, but did not have any effect on the non-actin binding mutant Phactr4*** (Fig. 6B). This shows that actin monomer levels can control the phosphorylation status of cofilin, and that Phactr4 acts downstream of actin monomers in this regulatory pathway. Significantly, depletion of Phactr4 by RNAi resulted in increased phospho-cofilin levels, when measured either by western blotting (Fig. 6C) or from individual cells by immunofluorescence (Fig. 6D,E). Importantly, in Phactr4 depleted cells expression of R62D failed to increase p-cofilin levels (Fig. 6F). This demonstrates the requirement for

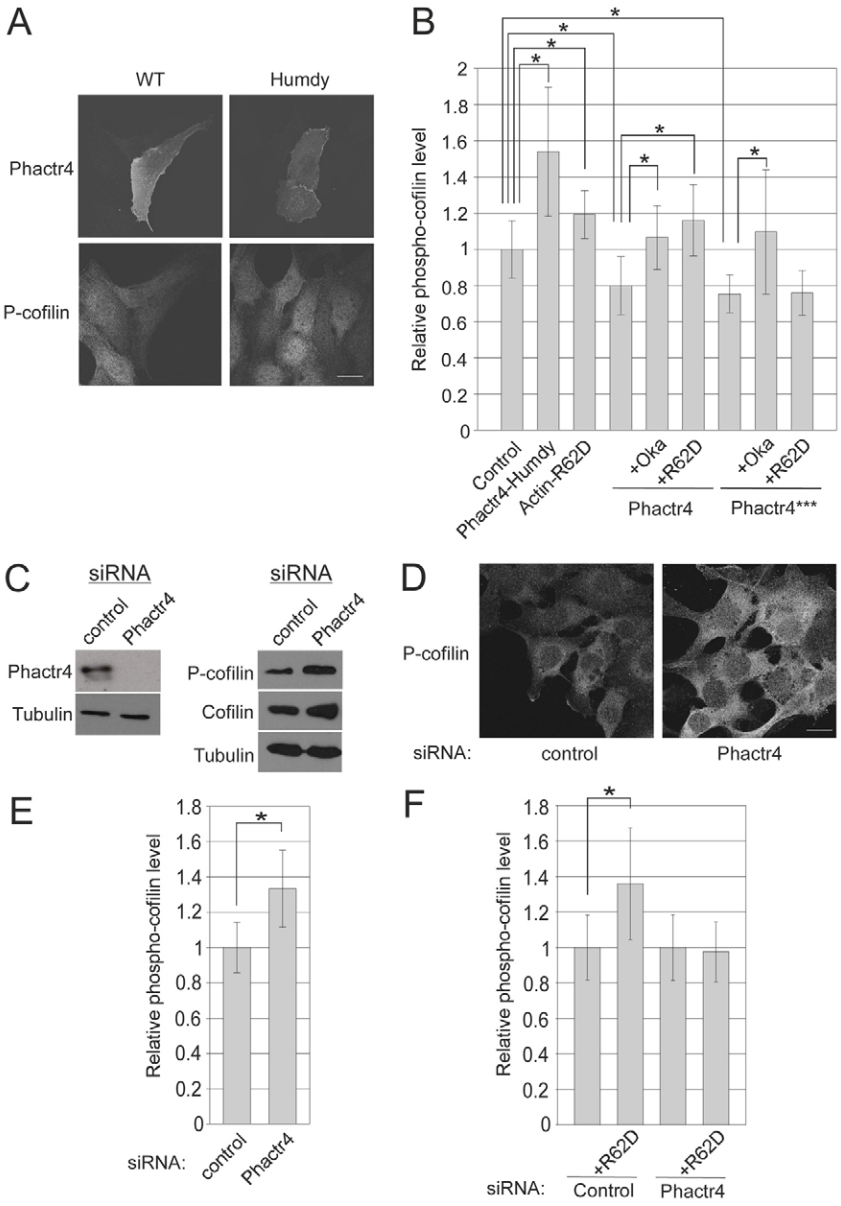

Fig. 6. Phactr4 regulates cofilin activity. (**A**) Confocal microscopy images of NIH 3T3 cells expressing FLAG-tagged Phactr4 (WT) or Phactr4-humdy (Humdy). Lower panels shows corresponding phospho-cofilin (P-cofilin) staining. (**B**) Relative levels of phosphorylated cofilin quantified from immunofluorescence images of cells transfected with indicated Phactr4 constructs with or without mCherry-actin-R62D (R62D) plasmids, with or without 30 minutes of 1 μM okadaic acid treatment (Oka). Data represent the mean intensity in at least 20 cells per condition from at least two independent experiments. (**C**) Western blot analysis of indicated proteins from cells transfected with control or Phactr4 siRNAs. (**D**) Confocal microscopy images with exactly the same imaging parameters from NIH 3T3 cells transfected with control or Phactr4 siRNAs, stained with phospho-cofilin (P-cofilin) antibody. (**E**) Quantification of relative phospho-cofilin levels in cells transfected with control or Phactr4 siRNAs. Data represent the mean intensity of at least 30 cells per condition from at least two independent experiments. (**F**) Relative levels of phosphorylated cofilin quantified from immunofluorescence images of cells transfected with the indicated siRNAs with or without FLAG-actin-R62D (R62D) plasmids. Data represents the mean of at least 30 cells from at least two independent experiments. Error bars indicate s.d., $*P<0.05$. Scale bars: 20 μm.

endogenous Phactr4 in regulating cofilin activity in response to actin monomer levels *in vivo*.

To assess whether Phactr4 could also regulate actin monomer levels in cells, we measured deoxyribonuclease I (DNase I) staining upon Phactr4 expression. Overexpression of both Phactr4 and Phactr4*** led to increased levels of actin monomers in cells, and the effect could be reversed by okadaic acid (Fig. 7A). Notably, this effect was dependent on cofilin activity, because Phactr constructs failed to increase the amount of actin monomers in cells depleted on cofilin (Fig. 7B,C). On the other hand, in line with the increased phospho-cofilin levels upon Phactr4-humdy mutant expression, these cells also displayed decreased DNase I staining (Fig. 7A). Mirroring the effects on actin monomers, the Phactr4 and Phactr4-humdy expressing cells displayed decreased and increased actin filament levels, respectively (Fig. 7D). These experiments suggest that Phactr4 may play a pivotal role in sensing the actin monomer levels in cells and transmitting this information through regulation of PP1 activity to cofilin, which is one of the key regulators of the actin monomer pool in cells.

Discussion

The balance between monomeric and filamentous actin in cells is crucial for many essential biological processes. Here we describe a previously uncharacterized regulatory mechanism by which the cell senses actin monomer amounts and acts to maintain them at appropriate levels. At the central stage of this feedback loop is Phactr4, which in response to decreased actin monomer-binding to its RPEL domain, guides PP1 to dephosphorylate and thus activate cofilin, a central actin disassembly factor (see Fig. 8 for model). Activation of cofilin will then replenish the actin monomer pool by depolymerization and severing of actin filaments. Our data therefore pinpoints a key role for the RPEL domain as a general actin monomer sensor in cells, which in the context of Phactr proteins modulates actin dynamics directly by affecting the activity status of a key actin regulator and which in

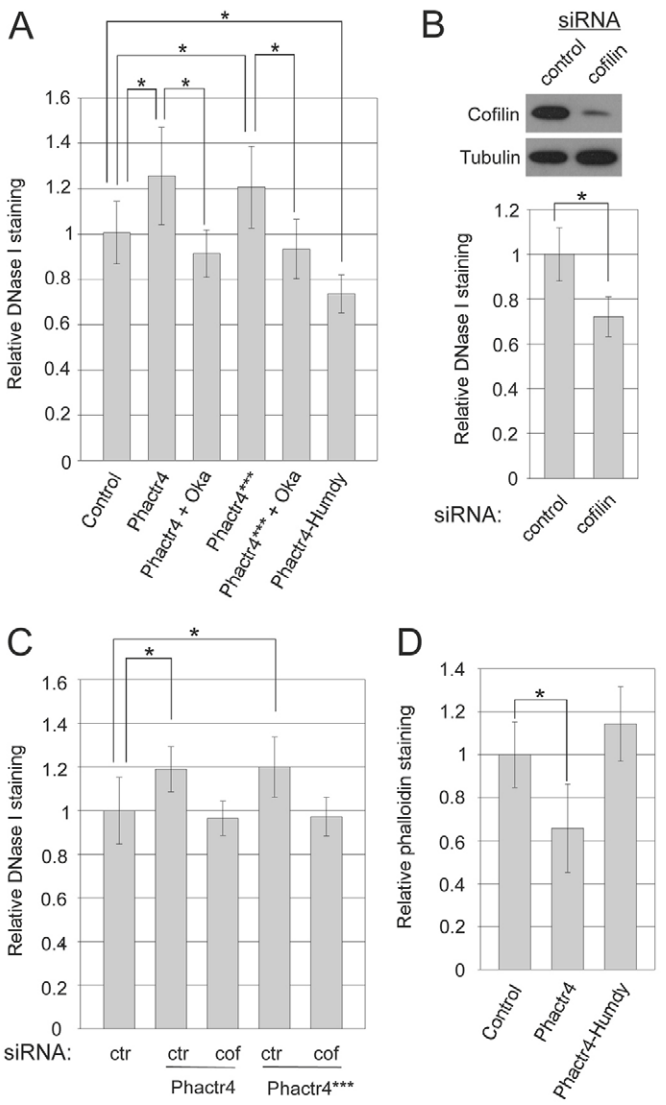

Fig. 7. Phactr4 regulates actin monomer levels in cells in response to actin dynamics. (**A**) Relative levels of actin monomers quantified from DNaseI-stained cells transfected with the indicated Phactr constructs with or without okadaic acid (Oka) treatment as in Fig. 6B. Data represent the mean of at least 24 cells per condition from at least two independent experiments. (**B**) Western blot analysis of indicated proteins in cells transfected with control or cofilin-1 siRNAs, and corresponding relative levels of actin monomers quantified with DNase I staining. Quantification data represent the mean intensity in at least 48 cells from at least two independent experiments. (**C**) Relative levels of actin monomers quantified from DNaseI-stained cells transfected with control (ctr) or cofilin-1 (cof) siRNAs and co-transfected with plasmids expressing Phactr4 or Phactr4***. See Materials and Methods for data normalization. Data represents the mean of at least 26 cells from at least two independent experiments. (**D**) Relative levels of actin filaments quantified from phalloidin-stained cells transfected or not with Phactr4 or Phactr4-humdy plasmids. Data represents the mean of at least 23 cells from at least two independent experiments. Error bars indicate s.d., $*P<0.05$.

the context of MRTFs regulates actin dynamics through transcriptional control of cytoskeletal genes (Fig. 8).

Phactr and MRTF family members are so far the only characterized protein families that possess an RPEL domain, which binds actin. Most of the amino acids that directly contact actin in the RPEL domain of MRTF-A in the published crystal structures (Hirano and Matsuura, 2011; Mouilleron et al., 2011) are conserved in the RPEL domains of Phactr proteins (Fig. 1B). Also the fact that mutations on the same residues disrupt the binding of both MRTF-A (Vartiainen et al., 2007) and Phactr4 (Fig. 4) to actin, support the notion of similar actin-binding mechanism between these proteins but in the absence of structural data on the Phactr-actin complex, this idea remains to be validated.

In addition to binding actin, the RPEL domain has also been implicated in regulating the nucleo-cytoplasmic shuttling of MRTFs (Guettler et al., 2008). Our data on both the full length protein as well as on the isolated RPEL domain (Fig. 2) demonstrate that the RPEL domain does not play a role in controlling the localization of Phactr4. This difference between MRTFs and Phactr4 is initially a bit puzzling as their RPEL domains are very similar. However, in the RPEL domain of Phactr4 there are two deletions at the level of the α-helices α3 and α5 in MRTF-A-RPEL (Mouilleron et al., 2011) (Fig. 1B). The deletion in the helix α5 corresponds to the B2 region, which is part of the bipartite NLS in MRTF-A (Pawlowski et al., 2010). In addition, one basic residue (K53) of the B3 domain in the RPEL domain of MRTF-A is replaced by non-basic residues in the four Phactr proteins (Fig. 1B). These differences may explain why we observed only weak binding of Phactr4 RPEL domain to the nuclear import receptors known to mediate nuclear import of MRTF-A (Pawlowski et al., 2010). Consequently, the localization of Phactr4 does not respond to the same actin perturbing stimuli as MRTF-A does (Fig. 2). Similarly, it has been reported that in rat cortical neurons the localization of Phactr1 does not respond to Latrunculin A or Cytochalasin D treatments (Farghaian et al., 2011). Our FRAP experiments suggested that there is continuous import of Phactr4 to the nucleus (Fig. 2E) and that this import is likely active, because the size of the fusion construct used in these studies (GFP-Phactr4, 104 kDa) puts it well beyond the nuclear pore diffusion limit (Keminer and Peters, 1999; Paine et al., 1975). The continuous import suggests that there is also continuous export as bulk of the protein remains localized to the cytoplasm. The export is likely not mediated by Crm1, because leptomycin B treatment did not have any effect on Phactr4 localization (Fig. 2C,D). The exact sequences and mechanisms mediating nuclear transport of Phactr4 remain to be determined.

Instead of regulating Phactr4 localization, we reveal here that actin-binding to the RPEL domain influences the ability of Phactr4 to activate PP1 through a competition mechanism. Structurally, the PP1 binding tail begins right after the Phactr4 RPEL domain. The close spatial proximity by itself could easily explain the competition. These findings suggest that release of Phactr4 from bound actin monomers can liberate it to activate PP1.

PP1 is one of the main dephosphorylating enzymes in the cell, with numerous substrates and cellular processes dependent on it. The activity of the PP1 catalytic subunit is regulated by a large number of targeting subunits, which confer the substrate, localization and temporal specificity to PP1 actions (Bollen et al., 2010). It is thought that Phactr proteins act as such targeting subunits but only few substrates for this dephosphorylation pathway have been described so far. Studies on the *humdy* mouse mutant have revealed abnormal phosphorylation of both the cell cycle regulator retinoblastoma

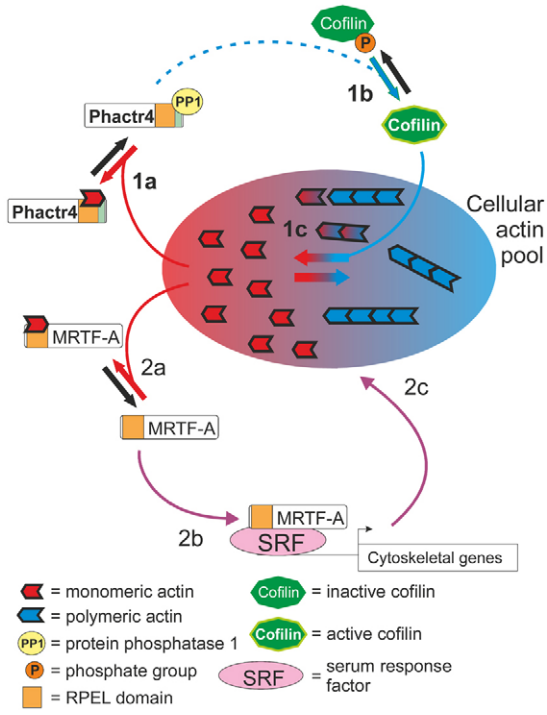

Fig. 8. Model depicting regulatory circuits by the RPEL domain containing proteins Phactr4 and MRTF-A that maintain cellular actin balance. (1a) Actin monomers and PP1 binding compete for binding to Phactr4. At high actin monomer levels, actin-binding to the RPEL domain (orange box in both Phactr4 and MRTF-A) of Phactr4 obstructs PP1 binding to Phactr4. However, lowered actin monomer concentration enables actin-free Phactr4 to bind PP1, activating it. (1b) PP1 then directly or indirectly dephosphorylates and activates cofilin, enabling the depolymerization and severing activity inherent for this protein. (1c) Action of cofilin on filamentous actin results in the restoration of actin monomer pool and discontinuation of Phactr4-mediated cofilin activation signals. (2a) Actin monomer-binding to the RPEL domain regulates the nuclear localization and activity of MRTF-A. At high actin monomer levels, the actin-bound RPEL domain in MRTF-A keeps the transcription factor in continuous transport between the nucleus and the cytoplasm, and prevents it from activating SRF. (2b) Upon loss of actin-binding, MRTF-A is retained in the nucleus, where it activates SRF. (2c) SRF activation results in the expression of several genes intimately connected to the cytoskeleton. MRTF-A data are based on published material (Vartiainen et al. 2007).

protein (Kim et al., 2007) and the actin severing protein cofilin (Zhang et al., 2012). Our data indicates that Phactr4 can regulate cofilin phosphorylation in response to actin dynamics (Fig. 6). Interestingly, the notion that actin monomer levels would regulate cofilin phosphorylation was raised already in 1997 (Minamide et al., 1997) but the mechanism was not elucidated. One of the main functions of cofilin in cells is to sever and depolymerise actin filaments and thereby replenish the actin monomer pool. The activity of cofilin can be regulated by phosphorylation on serine-3, which inhibits actin-binding. In addition to the cofilin 'specific' LIM (Arber et al., 1998) and TES kinases (Toshima et al., 2001), as well as slingshot (Niwa et al., 2002) and chronophin (Gohla et al., 2005) phosphatases, also the 'general' protein phosphatases PP1, PP2A and PP2B (Ambach et al., 2000; Meberg et al., 1998) have been reported to dephosphorylate cofilin. This seems to be important for example in T cells (Ambach et al., 2000) and upon cell motility inhibition caused by ALDH1L1 (Oleinik et al., 2010). Despite this reported direct link between cofilin and PP1, we cannot exclude the possibility that the actin-Phactr-PP1 axis reported here would affect some upstream components of the cofilin regulatory pathway, because for example both LIM kinase and slingshot are phospho-proteins (Van Troys et al., 2008). Therefore, in the future, it will be interesting to assess how the actin-regulated dephosphorylation pathway for cofilin depicted here is integrated with the other activation pathways described for this central actin regulator.

Our results suggest that PP1-mediated dephosphorylation of cofilin can function as a general mechanism to fine-tune actin monomer levels in cells. Although we were able to evoke measurable changes in both phospho-cofilin and actin monomer levels at the level of the whole cell (Figs 6 and 7), it is possible that under normal circumstances this pathway operates very locally to fine-tune actin monomer levels for example at the leading edge of a motile cell. This hypothesis is supported by our observations that Phactr4 is targeted to the plasma membrane through its N-terminal region (Fig. 3), which is likely not going to interfere with its ability to bind actin or PP1. Cofilin and Phactr4 have also been shown to colocalize at the edge of the lamellipodium of migrating mouse embryonic fibroblasts (Zhang et al., 2012). Defects in the regulation of the actin monomer pool may therefore also explain the findings that many Phactr family members seem to be required for cell motility (Sagara et al., 2009; Zhang et al., 2012).

In addition to the local role at the leading edge described above, it is also of interest to speculate a purpose for the considerable cytosolic and nuclear presence of the Phactr family proteins (Fig. 2), especially since also PP1 is found at these cellular sites (Andreassen et al., 1998). The described feedback loop via cofilin phosphorylation might cause, for example, fluctuations in nucleo-cytoplasmic transport of actin, as dephosphorylated cofilin has been shown to be required for nuclear import of actin (Dopie et al., 2012). Alternatively, this mechanism could also function in the nucleus to regulate gene expression, as both actin (Dopie et al., 2012; Hofmann et al., 2004; Philimonenko et al., 2004) and cofilin (Obrdlik and Percipalle, 2011) have reported roles during transcription. Therefore, Phactr proteins could be yet another example of information transmission between the actin pools in the nucleus and the cytoplasm. Nevertheless, it is also likely that in addition to regulating the phosphorylation status of cofilin, Phactr4 could also affect other PP1 targets. Detailed analysis of the PP1 substrates targeted by Phactr proteins is required to fully comprehend how they modulate various cellular processes.

This work highlights the role of the RPEL domain as a general sensor for the actin monomer levels in the cell. Essentially the same mechanisms seem to govern the regulation of both MRTF-A and Phactr4 by actin. In both cases, actin-binding to the RPEL domain prevents the interaction with another protein. In the case of MRTF-A, actin-binding masks an NLS and thus prevents the access of nuclear import factors (Hirano and Matsuura, 2011; Mouilleron et al., 2011). In the case of Phactr4, actin-binding prevents the PP1 binding and activation (Fig. 5). The downstream events are then very different, with MRTF-A activating SRF-mediated transcription and Phactr4 modulating cofilin phosphorylation. Nevertheless, both of these pathways converge again at the level of regulating actin dynamics, as many SRF targets are cytoskeletal genes and cofilin is a key regulator

of actin dynamics. In principle, both of these regulatory pathways respond to the same stimulus: decreased actin monomer levels in the cell. The response evoked by Phactr4 on cofilin activity is likely to be more rapid than the transcription response elicited by MRTF-A. This raises the idea that maybe these two pathways are differentially sensitive to changes in actin monomer levels. Binding of actin to the RPEL domain is quite complex, which is highlighted by the fact that structural studies with MRTF-A have revealed complexes with either three or five actin monomers (Mouilleron et al., 2008; Mouilleron et al., 2011). Moreover, the actual MRTF-A-actin configuration in cells as well as the functional properties of the complexes with different actin stoichiometrics remain unclear. It is nevertheless tempting to speculate that perhaps only small changes in the actin monomer pool will permit PP1 binding to Phactr4, by for example releasing the actin only from the RPEL motif 3, which is adjacent to the PP1-binding tail. This would then permit modulation of local fluctuations in the actin monomer pool, e.g. at the leading edge of a motile cell. In contrast, MRTF-A may require more substantial decrease in the monomer pool to permit access to the NLS, which is buried within the RPEL domain. Thereby only extensive changes in the actin monomer pool, which cannot be corrected by simple modulation of cofilin activity, would evoke a transcriptional response. Alternatively, also other signals may contribute to the regulation, and for example both Phactr proteins (Farghaian et al., 2011) and MRTF-A (Muehlich et al., 2008) have been shown to be phosphorylated in cells. Structural studies on the Phactr4-actin complex, as well as development of methods to both measure and perturb the different stoichiometric complexes between the RPEL domain and actin, in the context of both MRTF and Phactr proteins, are required to resolve these questions.

During the revision of this manuscript, Wiezlak et al. reported that another Phactr-family member, Phactr1, also binds actin and PP1 in a competitive manner and that this mechanism is used in cells to regulate acto-myosin assembly (Wiezlak et al., 2012). This emphasizes the roles of Phactr-proteins as actin monomer-sensors that can then regulate various cellular processes through PP1 in response to actin dynamics.

Materials and Methods

Plasmids and antibodies

Details of the DNA constructs cloned for this study are available upon request. The Phactr constructs used in the study are indicated in Fig. 1C. Plasmids that have been previously described include: pEF-FLAG-MRTF-A-RPEL-PK (Guettler et al., 2008), MRTF-A-GFP, MRTF-A***-GFP, GST-MRTF-A-1–204 (Vartiainen et al., 2007) and p3DA.luc (Geneste et al., 2002). mCherry-CAAX (van Rheenen et al., 2007) was a kind gift from Jacco van Rheenen, pQE-RanQ69L from Dr Dirk Görlich and pRL-TK was from Promega.

The following antibodies were from Sigma-Aldrich (St Louis): FLAG (M2), HRP-conjugated FLAG (M2), HRP-conjugated HA (HA-7), β-actin (AC-15), importin β (31H4), importin α (I1784). Crm1/Exportin-1 antibody was from BD Transduction Laboratories and cofilin (phospho-Ser3) antibodies were from Signalway Antibody and Cell Signalling. The following secondary antibodies were from Invitrogen: HRP-conjugated anti-mouse, HRP-conjugated anti-rabbit, Alexa-Fluor-647-conjugated anti-mouse, Alexa-Fluor-488-conjugated anti-rabbit, Alexa-Fluor-488-conjugated anti-mouse and Alexa-Fluor-594-conjugated anti-mouse.

Cell culture, transfections, cell staining and microscopy

The mouse fibroblast NIH 3T3 cell line was grown at 37℃, 5% CO_2 in Dulbecco's modified medium supplemented with 10% fetal calf serum (Gibco/Invitrogen) and antibiotics (penicillin/streptomycin, Gibco/Invitrogen). For plasmid transfections, Turbofect (Fermentas), Lipofectamine™ or Lipofectamine 2000™ (Invitrogen) were used according to manufacturer's instructions. The amounts of plasmids varied from 10 ng to 100 ng on a 24-well format depending on the application. After 24 hours and where indicated, cells were treated with 15% fetal calf serum, 0.5 μM latrunculin B (Sigma), 2 μM cytochalasin D (Sigma), 20 nM leptomycin B (Calbiochem) or 1 μM okadaic acid (Sigma) for indicated times before processing the samples.

For RNA interference experiments, cells were transfected with 10 nM gene specific siRNAs mouse cofilin 1 (Dopie et al. 2012); mouse Phactr4: 5′-GUAACUGAUGCUCAUGACU-3′ and 5′-CCUGAAUUCUUGGCCUUGU-3′ (Sigma) or AllStars Negative Control (Qiagen) using Interferin (Polyplus). Cells were re-transfected on day 3 with 10 nM siRNA and, when indicated with 100 ng of plasmids, using jetPRIME transfection reagent (Polyplus), then incubated overnight, and processed.

The import assays was performed as described in Dopie et al. (Dopie et al., 2012). Transfected cells grown on coverslips were fixed and immunostained with antibodies. When applicable, cells were also stained with DAPI (Sigma), Alexa-Fluor-488- or 594-conjugated phalloidin (Molecular Probes) or Alexa-Fluor-594-conjugated DNaseI (Invitrogen). Cells were imaged with Zeiss Imager M2 fluorescence microscope equipped with Axio Cam HRm camera and AxioVision software using 63× 1.4 objective. For RNAi experiments, the images were acquired using the same exposure time. The fluorescence intensities of Alexa-Fluor-conjugated DNaseI and antibody stained phospho-cofilin were quantified using ImageJ. In each image, the average intensity of the transfected cell was normalized to the intensity of a neighbouring non-transfected cell to exclude variations from staining efficiency and image acquisition. As the data conformed to normal distribution, the statistical analysis was performed with two-tailed Student's *t*-test, with two-sample unequal variance.

FRET/FLIM

Förster resonance energy transfer (FRET) measurements were carried out with Leica SP5 confocal microscope (Leica Microsystems, Germany) controlled by the LAS AF software, with the TiSa MaiTai HP 690–1040 nm multiphoton laser, using a glycerol immersion objective, model HCX APO 63× 1.30 Corr CS 21, and the PicoHarp 300 (PicoQuant, Germany) instrument for photon detection. Lifetime images were recorded with 256×256 image format, using the scanning speed of 200 Hz until the brightest pixel had at least 1000 counts. The average lifetime of the GFP was calculated by first manually segmenting the cells, and then fitting one exponential decay curve to the lifetime histograms. Binning mask of 6×6 was applied to ensure that each pixel contained at least 5000 counts. FRET efficiency was calculated as $E=(1-\tau DA/\tau D)\times 100$ (τDA average donor lifetime in presence of acceptor; τD average donor lifetime without acceptor).

Co-immunoprecipitation assays

NIH 3T3 cells were transfected by using Lipofectamine 2000 with plasmids expressing the appropriate HA- or FLAG-tagged proteins (3 μg each plasmid on a 10 cm dish). Forty eight hours later, cells were harvested in immunoprecipitation (IP) buffer (0.5% Triton X-100, 50 mM Tris-HCl pH 7.5, 150 mM NaCl), supplemented with Protease inhibitor cocktail (Roche). Lysate was cleared by centrifugation, diluted 1:2 with IP buffer without Triton X-100, applied on 25 μl of FLAG M2 antibody-coated beads or EZview Red Anti-HA Affinity Gel (Sigma-Aldrich), incubated for 2 hours and washed three times in IP buffer. Finally, the samples were boiled in SDS-PAGE loading buffer and resolved by SDS-PAGE, followed by western blotting with indicated antibodies.

Luciferase reporter assays

The NIH3T3 cells were transfected with appropriate mutant or wild-type Phactr4 constructs and co-transfected with the SRF-responsive p3DA-luc and constitutively active pRL-TK-luc (Promega) reporter plasmids. After 24 hours, the cells were harvested and analyzed with the Dual-Luciferase reporter assay system (Promega) and a luminometer according to manufacturer's directives. For each sample, the activity of firefly luciferase was normalized to the renilla luciferase activity.

GST-pulldown

His- tagged Ran-Q69L was purified as described in Görlich et al. (Görlich et al., 1994). For GST pull-downs, glutathione-agarose beads (Macherey-Nagel) were saturated with GST-Ph4-529–694 or GST-MRTF-A-1–204 derivatives from bacterial lysates. The beads were then incubated with 200 μl of cytoplasmic HeLa cell lysate in 50 mM NaCl, 0,02% Triton X-100, together with an energy mix (20 mM phosphocreatine, 1 mM GTP, 1 mM ATP, 50 μg/ml creatine phosphokinase), and with/without 50 μM Ran-Q69L for 3 hours at 4℃. After incubation, beads were washed three times with 10 mM HEPES (pH 8), 1,5 mM $MgCl_2$, 10 mM KCl, 0,02% Triton X-100) and eluted in SDS-PAGE loading buffer. Boiled samples were resolved on SDS-PAGE and subjected for western blotting with indicated antibodies.

PP1 phosphatase assay

The activity of PP1 catalytic subunit (Sigma Aldrich) was measured using the colorimetric SensoLyte pNPP Protein Phosphatase Assay Kit (Ana Spec) according to manufacturer's instruction with Varioskan platereader

(ThermoScientific). Actin was prepared from rabbit skeletal muscle as described in Pardee and Spudich (Pardee and Spudich, 1982).

Acknowledgements

We thank members of the Vartiainen laboratory for critical reading of this manuscript. Johanna Puusaari is acknowledged for technical assistance. Imaging was performed at the Light Microscopy Unit, Institute of Biotechnology.

Funding

This work was funded by Academy of Finland, University of Helsinki research funds, Sigrid Juselius foundation and Finnish Cancer Foundations. K.-P.S. and J.D. are funded by a fellowship from the Viikki Graduate School in Biosciences and the Helsinki Graduate Program in Biotechnology and Molecular Biology, respectively. Deposited in PMC for immediate release.

References

Allain, B., Jarray, R., Borriello, L., Leforban, B., Dufour, S., Liu, W. Q., Pamonsinlapatham, P., Bianco, S., Larghero, J., Hadj-Slimane, R. et al. (2012). Neuropilin-1 regulates a new VEGF-induced gene, Phactr-1, which controls tubulogenesis and modulates lamellipodial dynamics in human endothelial cells. *Cell. Signal.* **24**, 214-223.

Allen, P. B., Greenfield, A. T., Svenningsson, P., Haspeslagh, D. C. and Greengard, P. (2004). Phactrs 1-4: A family of protein phosphatase 1 and actin regulatory proteins. *Proc. Natl. Acad. Sci. USA* **101**, 7187-7192.

Ambach, A., Saunus, J., Konstandin, M., Wesselborg, S., Meuer, S. C. and Samstag, Y. (2000). The serine phosphatases PP1 and PP2A associate with and activate the actin-binding protein cofilin in human T lymphocytes. *Eur. J. Immunol.* **30**, 3422-3431.

Andreassen, P. R., Lacroix, F. B., Villa-Moruzzi, E. and Margolis, R. L. (1998). Differential subcellular localization of protein phosphatase-1 alpha, gamma1, and delta isoforms during both interphase and mitosis in mammalian cells. *J. Cell Biol.* **141**, 1207-1215.

Arber, S., Barbayannis, F. A., Hanser, H., Schneider, C., Stanyon, C. A., Bernard, O. and Caroni, P. (1998). Regulation of actin dynamics through phosphorylation of cofilin by LIM-kinase. *Nature* **393**, 805-809.

Bollen, M., Peti, W., Ragusa, M. J. and Beullens, M. (2010). The extended PP1 toolkit: designed to create specificity. *Trends Biochem. Sci.* **35**, 450-458.

Dopie, J., Skarp, K. P., Rajakylä, E. K., Tanhuanpää, K. and Vartiainen, M. K. (2012). Active maintenance of nuclear actin by importin 9 supports transcription. *Proc. Natl. Acad. Sci. USA* **109**, E544-E552.

Farghaian, H., Chen, Y., Fu, A. W., Fu, A. K., Ip, J. P., Ip, N. Y., Turnley, A. M. and Cole, A. R. (2011). Scapinin-induced inhibition of axon elongation is attenuated by phosphorylation and translocation to the cytoplasm. *J. Biol. Chem.* **286**, 19724-19734.

Favot, L., Gillingwater, M., Scott, C. and Kemp, P. R. (2005). Overexpression of a family of RPEL proteins modifies cell shape. *FEBS Lett.* **579**, 100-104.

Fornerod, M., Ohno, M., Yoshida, M. and Mattaj, I. W. (1997). CRM1 is an export receptor for leucine-rich nuclear export signals. *Cell* **90**, 1051-1060.

Geneste, O., Copeland, J. W. and Treisman, R. (2002). LIM kinase and Diaphanous cooperate to regulate serum response factor and actin dynamics. *J. Cell Biol.* **157**, 831-838.

Gohla, A., Birkenfeld, J. and Bokoch, G. M. (2005). Chronophin, a novel HAD-type serine protein phosphatase, regulates cofilin-dependent actin dynamics. *Nat. Cell Biol.* **7**, 21-29.

Görlich, D., Prehn, S., Laskey, R. A. and Hartmann, E. (1994). Isolation of a protein that is essential for the first step of nuclear protein import. *Cell* **79**, 767-778.

Görlich, D., Panté, N., Kutay, U., Aebi, U. and Bischoff, F. R. (1996). Identification of different roles for RanGDP and RanGTP in nuclear protein import. *EMBO J.* **15**, 5584-5594.

Guettler, S., Vartiainen, M. K., Miralles, F., Larijani, B. and Treisman, R. (2008). RPEL motifs link the serum response factor cofactor MAL but not myocardin to Rho signaling via actin binding. *Mol. Cell. Biol.* **28**, 732-742.

Hirano, H. and Matsuura, Y. (2011). Sensing actin dynamics: structural basis for G-actin-sensitive nuclear import of MAL. *Biochem. Biophys. Res. Commun.* **414**, 373-378.

Hofmann, W. A., Stojiljkovic, L., Fuchsova, B., Vargas, G. M., Mavrommatis, E., Philimonenko, V., Kysela, K., Goodrich, J. A., Lessard, J. L., Hope, T. J. et al. (2004). Actin is part of pre-initiation complexes and is necessary for transcription by RNA polymerase II. *Nat. Cell Biol.* **6**, 1094-1101.

Jarray, R., Allain, B., Borriello, L., Biard, D., Loukaci, A., Larghero, J., Hadj-Slimane, R., Garbay, C., Lepelletier, Y. and Raynaud, F. (2011). Depletion of the novel protein PHACTR-1 from human endothelial cells abolishes tube formation and induces cell death receptor apoptosis. *Biochimie* **93**, 1668-1675.

Kalderon, D., Roberts, B. L., Richardson, W. D. and Smith, A. E. (1984). A short amino acid sequence able to specify nuclear location. *Cell* **39**, 499-509.

Keminer, O. and Peters, R. (1999). Permeability of single nuclear pores. *Biophys. J.* **77**, 217-228.

Kim, T. H., Goodman, J., Anderson, K. V. and Niswander, L. (2007). Phactr4 regulates neural tube and optic fissure closure by controlling PP1-, Rb-, and E2F1-regulated cell-cycle progression. *Dev. Cell* **13**, 87-102.

Meberg, P. J., Ono, S., Minamide, L. S., Takahashi, M. and Bamburg, J. R. (1998). Actin depolymerizing factor and cofilin phosphorylation dynamics: response to signals that regulate neurite extension. *Cell Motil. Cytoskeleton* **39**, 172-190.

Minamide, L. S., Painter, W. B., Schevzov, G., Gunning, P. and Bamburg, J. R. (1997). Differential regulation of actin depolymerizing factor and cofilin in response to alterations in the actin monomer pool. *J. Biol. Chem.* **272**, 8303-8309.

Miralles, F., Posern, G., Zaromytidou, A. I. and Treisman, R. (2003). Actin dynamics control SRF activity by regulation of its coactivator MAL. *Cell* **113**, 329-342.

Mouilleron, S., Guettler, S., Langer, C. A., Treisman, R. and McDonald, N. Q. (2008). Molecular basis for G-actin binding to RPEL motifs from the serum response factor coactivator MAL. *EMBO J.* **27**, 3198-3208.

Mouilleron, S., Langer, C. A., Guettler, S., McDonald, N. Q. and Treisman, R. (2011). Structure of a pentavalent G-actin*MRTF-A complex reveals how G-actin controls nucleocytoplasmic shuttling of a transcriptional coactivator. *Sci. Signal.* **4**, ra40.

Muehlich, S., Wang, R., Lee, S. M., Lewis, T. C., Dai, C. and Prywes, R. (2008). Serum-induced phosphorylation of the serum response factor coactivator MKL1 by the extracellular signal-regulated kinase 1/2 pathway inhibits its nuclear localization. *Mol. Cell. Biol.* **28**, 6302-6313.

Niwa, R., Nagata-Ohashi, K., Takeichi, M., Mizuno, K. and Uemura, T. (2002). Control of actin reorganization by Slingshot, a family of phosphatases that dephosphorylate ADF/cofilin. *Cell* **108**, 233-246.

Obrdlik, A. and Percipalle, P. (2011). The F-actin severing protein cofilin-1 is required for RNA polymerase II transcription elongation. *Nucleus* **2**, 72-79.

Oleinik, N. V., Krupenko, N. I. and Krupenko, S. A. (2010). ALDH1L1 inhibits cell motility via dephosphorylation of cofilin by PP1 and PP2A. *Oncogene* **29**, 6233-6244.

Paavilainen, V. O., Bertling, E., Falck, S. and Lappalainen, P. (2004). Regulation of cytoskeletal dynamics by actin-monomer-binding proteins. *Trends Cell Biol.* **14**, 386-394.

Paine, P. L., Moore, L. C. and Horowitz, S. B. (1975). Nuclear envelope permeability. *Nature* **254**, 109-114.

Pardee, J. D. and Spudich, J. A. (1982). Purification of muscle actin. *Methods Cell Biol.* **24**, 271-289.

Pawłowski, R., Rajakylä, E. K., Vartiainen, M. K. and Treisman, R. (2010). An actin-regulated importin α/β-dependent extended bipartite NLS directs nuclear import of MRTF-A. *EMBO J.* **29**, 3448-3458.

Philimonenko, V. V., Zhao, J., Iben, S., Dingová, H., Kyselá, K., Kahle, M., Zentgraf, H., Hofmann, W. A., de Lanerolle, P., Hozák, P. et al. (2004). Nuclear actin and myosin I are required for RNA polymerase I transcription. *Nat. Cell Biol.* **6**, 1165-1172.

Sagara, J., Higuchi, T., Hattori, Y., Moriya, M., Sarvotham, H., Shima, H., Shirato, H., Kikuchi, K. and Taniguchi, S. (2003). Scapinin, a putative protein phosphatase-1 regulatory subunit associated with the nuclear nonchromatin structure. *J. Biol. Chem.* **278**, 45611-45619.

Sagara, J., Arata, T. and Taniguchi, S. (2009). Scapinin, the protein phosphatase 1 binding protein, enhances cell spreading and motility by interacting with the actin cytoskeleton. *PLoS ONE* **4**, e4247.

Sun, Q., Chen, G., Streb, J. W., Long, X., Yang, Y., Stoeckert, C. J., Jr and Miano, J. M. (2006). Defining the mammalian CArGome. *Genome Res.* **16**, 197-207.

Toshima, J., Toshima, J. Y., Amano, T., Yang, N., Narumiya, S. and Mizuno, K. (2001). Cofilin phosphorylation by protein kinase testicular protein kinase 1 and its role in integrin-mediated actin reorganization and focal adhesion formation. *Mol. Biol. Cell* **12**, 1131-1145.

van Rheenen, J., Song, X., van Roosmalen, W., Cammer, M., Chen, X., Desmarais, V., Yip, S. C., Backer, J. M., Eddy, R. J. and Condeelis, J. S. (2007). EGF-induced PIP2 hydrolysis releases and activates cofilin locally in carcinoma cells. *J. Cell Biol.* **179**, 1247-1259.

Van Troys, M., Huyck, L., Leyman, S., Dhaese, S., Vandekerkhove, J. and Ampe, C. (2008). Ins and outs of ADF/cofilin activity and regulation. *Eur. J. Cell Biol.* **87**, 649-667.

Vartiainen, M. K., Guettler, S., Larijani, B. and Treisman, R. (2007). Nuclear actin regulates dynamic subcellular localization and activity of the SRF cofactor MAL. *Science* **316**, 1749-1752.

Wiezlak, M., Diring, J., Abella, J., Mouilleron, S., Way, M., McDonald, N. Q. and Treisman, R. (2012). G-actin regulates shuttling and PP1 binding by the RPEL protein Phactr1 to control actomyosin assembly. *J. Cell Sci.* **125**, 5860-5872.

Zhang, Y., Kim, T. H. and Niswander, L. (2012). Phactr4 regulates directional migration of enteric neural crest through PP1, integrin signaling, and cofilin activity. *Genes Dev.* **26**, 69-81.